# Evaluating Sentinel-1 Capability in Classifying Dieback in Chestnut and Oak Forests

Florian Mouret, Marie Parrens, Véronique Cheret, Jean-Philippe Denux, Cécile Vincent-Barbaroux, Milena Planells

# Evaluating Sentinel-1 Capability in Classifying Dieback in Chestnut and Oak Forests

Florian Mouret, Marie Parrens, Véronique Chéret, Jean-Philippe Denux, Cécile Vincent-Barbaroux, Milena Planells

***Abstract*—This letter analyzes the contribution of the Sentinel-1 (S1) satellites, which provide C-band synthetic aperture radar (SAR) data, to the monitoring of forest dieback. Multispectral satellites (typically Landsat 8 or Sentinel-2, S2) have been found to be effective in detecting early signs of dieback, while little work has been done with SAR data despite its sensitivity to canopy structure and water content and its ability to pass through clouds. Our analysis is conducted on two study sites in France, where the dieback of chestnut and oak plots have been labeled. Classifications have been conducted to measure the ability of S1 data to identify plot in dieback. Our results show that S1 time series are not very sensitive to forest dieback. Using a single S2 images lead to more powerful classification results than using 1 year of S1 data. While S1 data may not be suitable for stand-alone forest dieback detection, it could be interesting to use it for other forest monitoring applications that should not be affected by dieback (species identification, clear-cut detection, etc.).**

***Index Terms*—Forest dieback detection, Sentinel-2, Sentinel-1, machine learning**

## I. Introduction

MONITORING the health of forests is important because they play a critical role in many aspects of the Earth's ecosystem (carbon cycle, biodiversity, water cycle) as well as other important economic and social functions. Climate change is expected to lead to an increase in droughts, abiotic and biotic disturbances, which will have a major impact on forest health [1]. This is for example the case in France, where an increase in forest dieback has been observed in recent years [2], [3]. Forest dieback is a complex phenomenon that results in the weakening of trees with loss of vigor, often without obvious direct causes. It arises from a combination of biotic (e.g., pathogens or insects) and abiotic (e.g., drought or pollution) factors, which may occur sequentially or simultaneously. Tree health decline can be slow and gradual (e.g., drought-induced dieback), generally visible as progressive crown and canopy loss over several years, or very rapid, resulting in mortality in a single year (e.g., bark beetle attacks). This study examines oak and chestnut forests, focusing on slow declines linked to drought and occasionally pathogens, such as blight in chestnuts, which are more challenging to detect due to their subtle nature. Traditional dieback assessment is typically conducted on small reference plots by assessing tree health (see details in Section II.B), and is therefore time-consuming and not suitable for covering large areas with fine resolution.

Remote sensing has been identified as a valuable tool to produce maps at large scale and fine resolution, especially since ground truth acquisition is challenging due to the scale of the areas to be analyzed. Such analyses have been facilitated by the Sentinel satellites, which are part of the European Union's Copernicus program and are freely available. In particular, recent studies have shown that using time series coming from the Sentinel-2 (S2) satellites are well suited to monitor forest health status [2], [4]. S2 satellites provide multispectral imagery with fine spatial (down to 10m) and temporal resolution (revisit time about 5 days in Europe), which is well suited for timely mapping of forest status. Moreover, the spectral response of S2 images is affected by forest dieback, especially in the shortwave infrared (SWIR) part of the spectrum, which correlates with the water content of the canopy [2].

In many applications, Sentinel-1 (S1) C-band synthetic aperture radar (SAR) data have shown good complementarity with S2 data [5]. In particular, S1 data are sensitive to canopy structure and water content [6] and are not affected by cloud cover [7]. However, investigating the interest of S1 data for forest dieback detection has received little attention in the literature. Some attention has been given to the detection of bark beetle attacks [8], however for this application the contribution of S1 when compared to S2 was not found significant [9]. More recently, [10] have shown that S1 data can be relevant for studying severe drought-induced damage (mainly associated with mortality) in hardwoods 2 years after the disturbance. However, foresters are interested to detect the first signs of tree dieback (before mortality) in order to collect the wood before it is damaged. Therefore, our study proposes to extend the analysis of the S1 data contribution to the early stages of dieback and to broadleaf forests, which have not been yet discussed.

In this letter, we focus on two case studies in France. The main objective is to automatically detect forest dieback (even in its very early stages) and over large areas using remote sensing data series. In particular, we want to assess whether the use of S1 data in comparison or in combination with S2 data is relevant for this purpose. The first use case is related to the drought-induced dieback of oak trees (*Quercus petraea*, *Quercus robur*), whose detailed analysis using only



Florian Mouret and Cécile Vincent-Barbaroux are with Université of Orléans, USC INRAE 1328 / P2E laboratory (Physiology, Ecology and Environment), BP 6759, rue de Chartres 45067 Cedex 2, Orléans, France (e-mail: florian.mouret; cecile.vincent1@univ-orleans.fr).

Florian Mouret, Marie Parrens and Milena Planells are with CESBIO, Université de Toulouse, CNES/CNRS/INRAE/IRD/UT3-Paul Sabatier, 18, Avenue Edouard Belin, 31401 Toulouse, France.

Marie Parrens, Véronique Chéret and Jean-Philippe Denux are with Dynafor, University of Toulouse, INRAE, INPT, INP-PURPAN, Castanet-Tolosan, France

S2 data has been carried out in [2]. The second use case is related to chestnut dieback (*Castanea sativa*) [11], which is mainly caused by both biotic (such as ink disease) and abiotic (drought) factors [12]. For both species, the dieback is relatively slow and subtle, i.e. the trees are weakened but can generally survive for several years (although the phenomenon can be more intense for chestnut).

## II. Study area and data

This section provides a description of the study sites, the reference data, labeling protocol and the satellite data used for our analysis.

### A. Study areas

The location of the oak and chestnut plots is depicted in Figure 1. The chestnut plots are located in the Nouvelle-Aquitaine region (2 S2 tiles) whereas the oak plots are located in the Centre-Val de Loire region and its surrounding (11 S2 tiles). Note that an S2 tile has an area of 10000km$^2$.

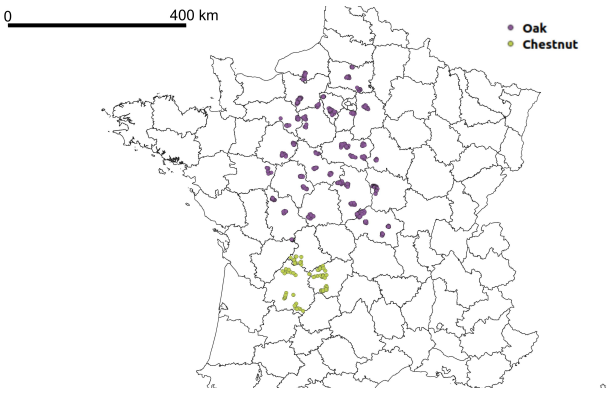


Fig. 1. Our two study sites are located in the Centre-Val de Loire region for oak (11 S2 tiles) and in the Nouvelle-Aquitaine region for chestnut (2 S2 tile).

### B. Reference data

The reference plots were labeled in 2020 for both oak and chestnut. The labeling protocol used is the DEPERIS protocol of the French Forest Health Service. This protocol assesses tree dieback by looking at the missing branches and ramifications (i.e., this is related to canopy loss). A plot is considered in dieback if more than 20% of its trees are in dieback. For more details on that point, we invite the readers to consult [2]. The chestnut dataset consists of 83 plots [11], of which 35 are labeled "healthy" (42%). The oak dataset is larger with 1685 plots, of which 1202 are labeled "healthy" (71.3%). For both species, plots are considered as "healthy" or "dieback" (two classes). Finally, as in [2], since we are working at the pixel level, all pixels of a plot are assigned the plot label.

### C. Sentinel data

*1) Sentinel-2:* For our analysis, we used a single synthetic S2 image taken in mid-July 2020. To have a unique image for each tile, we interpolated the S2 bands between the closest available images before and after July 15. The MAJA (Maccs-Atcor Joint Algorithm) processing chain was used to obtain Level 2A images with shadow and cloud masks, allowing us to have cloud-free data [13]. The 10 S2 bands (B) cover the visible (B2 to B4), red-edge (B5 to B7), near-infrared (NIR, B8 and B8a) and Shortwave Infrared (SWIR, B11 and B12) spectral regions. They were resampled to 10m (band 1, 9 and 10 are not adapted to vegetation monitoring and were excluded).

*2) Sentinel-1:* For our analysis, we used time series of S1 data collected between September 2019 and August 2020, included. We used the Level-1 Ground Range Detected (GRD) products. The S1 images were calibrated, orthorectified and corrected from slope effect using de s1tiling processing chain from Orfeo Toolbox[1]. The backscatter from the VH ($\sigma^0_{VH}$) and VV ($\sigma^0_{VV}$) polarizations are considered in this study, as well as indices presented in the Table I. The results presented in this paper were obtained using descending orbit data only. Monthly averaged features were computed to reduce noise and data dimensionality. Additional tests were also performed using both ascending and descending orbits, dense time series (without monthly averaging), and multi-temporal speckle-filtered data without changing our results.

TABLE I
Additional Sentinel-1 indices used in this study.

| Name (abbr.) | Formulation | Ref. |
|---|---|---|
| Backscatter intensity Ratio (ratio) | $\frac{\sigma^0_{VV}}{\sigma^0_{VH}}$ | [14] |
| Radar Vegetation Index (RVI) | $\frac{4\sigma^0_{VH}}{\sigma^0_{VV}+\sigma^0_{VH}}$ | [15] |
| Dual Polarization SAR VI (DPSVI) | $\frac{\sigma^0_{VV}+\sigma^0_{VH}}{\sigma^0_{VV}}$ | [16] |
| S-1 span (span) | $\sigma^0_{VV}+\sigma^0_{VH}$ | [10] |

## III. Methods

To assess the contribution of S1 data for forest dieback detection, we have conducted various analysis, which are summarized in Figure 2 and detailed in what follows. The main experiment is to compare classification results obtained using S1 data, S2 data, or a combination of S1 and S2 data. In addition, a feature importance analysis is conducted to further assess the contribution of S1 data. In order to robustly evaluate our results (classification and feature analysis), we used a repeated data splitting approach, i.e., the data was randomly split into training (70%) and test (30%) sets 30 times (the same selection is done for all the tested datasets). The splitting is done at the plot level, i.e. all pixel plots are in the same set, and the evaluation of the classification results is done at the plot level by taking the most frequent (mode) prediction.

### A. Dataset

The three dataset used for our analysis are composed as follows. Dataset S1 consists of S1 data only (72 features): monthly $\sigma^0_{VH}$, $\sigma^0_{VV}$, R, RVI, DPSVI and span were computed from September 2019 to August 2020. Dataset S2 consists of

[1]https://pypi.org/project/s1tiling/

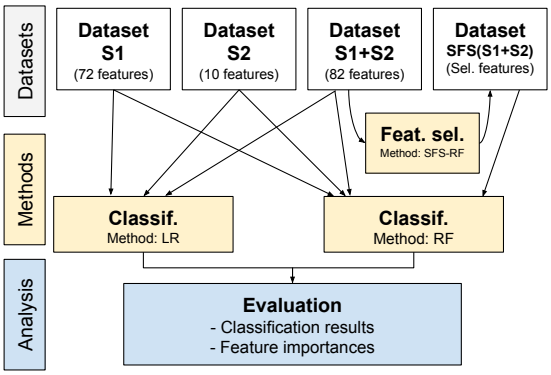


Fig. 2. Workflow of the different experiments carried out in our analysis. Feature selection methods (feat. sel.) are studied to identify the most important features for the two classification algorithms, Random Forest (RF) and Logistic Regression (LR).

S2 data only (10 features): only one S2 image (10 spectral bands) acquired in summer is used. Dataset S1+S2 combines dataset S1 and S2 (S1 and S2 data, 82 features). An additional dataset, SFS(S1+S2), is also considered and consists of a subset of dataset S1+S2 obtained after a feature selection using the Sequential Forward Selection (SFS), which is described in section III.C.2.

### B. Classification experiments

As a main baseline, we used the Random Forest (RF) algorithm to classify datasets S1, S2, and S1+S2 for chestnut and oak. Its robustness to overfitting and its ability to handle noisy, non-linear and high dimensional data make it a popular choice in remote sensing applications [17]. This choice was also motivated by the good results obtained in early work classifying forest dieback using S2 data [2]. RF was used to classify the plots in 2 classes: healthy or dieback. A minimal tuning of the algorithm was done by grid search based on the result obtained in [2] since RF is known to be very robust in the choice of its parameters. More precisely, to adapt the algorithm to the difference in number of samples of each dataset, we only changed the minimum number of samples in a node (5 for oaks and 30 for chestnut).

To investigate whether other strategies might provide complementary results, we performed a similar analysis using a linear classification model, i.e., logistic regression with the Least Absolute Shrinkage and Selection Operator (LASSO) penalty (the shrinkage coefficient was set to 0.1 via grid search for both species). The interest of these additional tests is twofold: 1) to ensure that using a different classification strategy (linear-based instead of tree-based) leads to the same conclusions, and 2) to have access to a different feature selection method. Since these additional tests did not bring novel conclusions to our analysis, they are only briefly discussed in Section IV. We used the Python library scikit-learn (version 1.2) for the implementation of both algorithms. Metrics used to evaluate the classification results are the overall accuracy (OA, percentage of samples correctly predicted), the Cohen's kappa (Kappa, the probability of agreement between predictions and ground-truth) and the macro F1 score (F1-macro, the average of the F1 score for each class). F1 score is the harmonic mean of the precision (number of true positives over true positives plus false positives) and the recall (number of true positives over true positives plus false negatives) and is not impacted by imbalanced datasets.

### C. Features selection and importance analysis

Dataset S1+S2 contains many features, correlation between them and data redundancy is likely. Feature selection methods aim to reduce the number of input variables by selecting only the most informative features that best capture the relevant information for the task, hence redundant or useless features are removed. In addition, they can give us some insight into the most informative features, which is often called feature importance and corresponds to features that are most powerful when used to solve the task at hand. We have tested 3 different methods on the dataset S1+S2, which are detailed below.

*1) RF feature importance:* the RF algorithm naturally provides feature importance, which reflects how much a feature contributed to the splitting decision during the training of the algorithm (it is computed as the normalized reduction in Gini impurity introduced by a feature during training). We took the average feature importance obtained after the 30 experiments.

*2) Sequential feature selection with RF algorithm:* despite the robustness of RF to high-dimensional data (demonstrated in our results), we used another feature selection method to identify the minimum number of features that could be used to have a near-optimal classification. The SFS algorithm [18] was used for that purpose. It is a greedy procedure that iteratively finds the best new feature to add to the set of selected features, based on an internal cross-validation score obtained using any classification estimator. In this procedure, we choose to optimize the F1-score at each iteration. Note that, as with our main train/test split experiment, to avoid autocorrelation and select relevant features, this internal cross-validation must be done by separating all pixels of the plot into the same sets. The main advantage of using SFS instead of the native impurity-based feature importance of the RF algorithm detailed above is that it is optimized on independent sets via the internal cross-validation, and thus avoids overfitting. Indeed, the built-in ranking of RF is derived from the training set, so the feature importance can be high even if the feature has no predictive power on independent testing data. Finally, the SFS algorithm is stopped if the classification metric (F1 score) does not improve by at least a small margin (0.001 in our case). This allows us to keep only the most significant features. The feature importance obtained after the 30 trials simply corresponds to the percentage of times a feature was selected.

*3) Feature selection via LASSO penalty:* when using logistic regression with a LASSO penalty (also known as l1 norm), the coefficient of useless or redundant features are set to zero. Moreover, features with larger influence tends to have larger absolute coefficient (the data need to be scaled in that case). The absolute coefficient values averaged after the 30 experiments are used as feature importance for this method.

TABLE II
OVERALL ACCURACY (OA), COHEN'S KAPPA AND F1 SCORE OBTAINED ON CHESTNUT AND OAK DATASETS WITH RF AND LR ALGORITHMS. ALL 95% CONFIDENCE INTERVAL ARE LOWER THAN 0.03 FOR CHESTNUT AND 0.001 FOR OAK. BEST VALUES ARE IN BOLD.

| Species | Dataset | Algorithm | OA | Kappa | F1 |
|---|---|---|---|---|---|
| Chestnut | S1 | RF | 0.50 | 0.01 | 0.49 |
| | S1 | LR | 0.48 | 0.01 | 0.47 |
| | S2 | RF | **0.90** | **0.8** | **0.90** |
| | S2 | LR | 0.87 | 0.74 | 0.87 |
| | S1+S2 | RF | **0.90** | 0.79 | **0.90** |
| | S1+S2 | LR | 0.86 | 0.73 | 0.86 |
| | S1+S2 | SFS-RF | 0.89 | 0.79 | 0.89 |
| Oak | S1 | RF | 0.71 | 0.02 | 0.44 |
| | S1 | LR | 0.63 | 0.22 | 0.6 |
| | S2 | RF | **0.77** | 0.37 | 0.68 |
| | S2 | LR | 0.69 | 0.36 | 0.67 |
| | S1+S2 | RF | 0.76 | 0.33 | 0.66 |
| | S1+S2 | LR | 0.71 | **0.39** | **0.69** |
| | S1+S2 | SFS-RF | 0.76 | 0.34 | 0.66 |

## IV. RESULTS AND DISCUSSION

### A. Classification results

The classification results obtained on the different datasets are summarized in Table II. Looking at these results, we can conclude that using S1 data only leads to poor results, especially when compared to using a single S2 image, for both oak and chestnut trees. In addition, combining S1 and S2 data (with or without feature selection) does not improve significantly the classification results. The best F1 score is obtained using RF with S2 or S1+S2 data for chestnut, while it is obtained using LR with S1+S2 data for oak (using only RF with S2 data provides very close accuracy). Overall, using the SFS algorithm is sufficient to reach a near-optimal accuracy, hence the feature selected with this method (see below) are sufficient to classify accurately our datasets. For oak, note that LR struggles to achieve good OA but obtains a good F1 score, which means that it can classify the minority class more accurately at the expense of reduced OA.

To complement these results, we should highlight the fact that only one S2 image is used in our analysis, further weakening the contribution of the S1 data. As pointed out in [2], using dense S2 time series can improve the early detection of forest dieback. Moreover, we conducted additional tests on the fusion of S1 and S2 data, including late fusion of S1 and S2 classifications using various methods (e.g., mean score, product of expert, and stacking), since previous studies have indicated that directly using all S1 and S2 features as input for the RF algorithm can be suboptimal [5]. However, even in this case, the low contribution of S1 data was confirmed by our experimental results.

While our analysis highlight the low sensitivity of S1 data to detect early signs of dieback, the results obtained in [10] indicate that it can still be useful for long-term monitoring to detect the most damaged areas and tree mortality in deciduous forests. Our results are consistent with those obtained in [9] for the detection of bark beetle attack (which has a stronger effect than drought-induced dieback). In their study, the authors observed that the S1 was affected by bark beetle attacks, but not enough to provide a good separation between healthy and declining plots. In addition, [19] emphasized the interest of S1 to detect clear cuts without being affected by dieback, which is also consistent with our results.

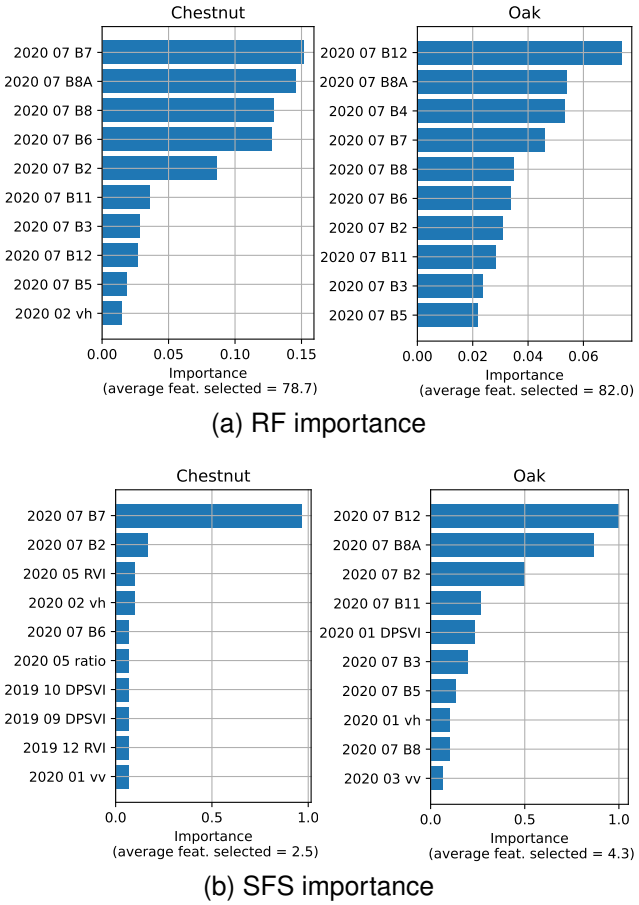


Fig. 3. Feature importance obtained for chestnut and oak plots with dataset S1+S2 using (a) the native RF feature importance and (b) the percentage of times a feature was selected using the SFS method. Feature names are displayed with the acquisition dates (year/month). The average number of features selected in each run is shown in parentheses for each method.

### B. Feature importance

The feature importance obtained with the RF and SFS-RF methods are displayed in Figure 3, along with the average number of features selected in each run. Overall, we can observe that S2 features are largely favored over S1 features, which is coherent with the classification results. In particular, S2 bands 7 and 8A are the most important to detect chestnut dieback, while B12 and B8A are the most important to detect oak dieback. When looking at the feature selected using the SFS method, we can notice that only few features are sufficient to detect forest dieback accurately. In particular, B7 is almost always selected to detect chestnut dieback (for SFS the importance is equal to the average number of times a feature is selected), while B12 and B8A are almost always selected for oak. Our results indicate that S2 bands B7 and B8A, which correlate with canopy chlorophyll content, are primarily used to detect chestnut dieback. In addition to B8A, band B12, which correlates with canopy water content, is also important for the detection of oak dieback. This finding is

consistent with the results reported in [2], where red-edge, NIR and SWIR portions of the S2 spectrum were found to be important for monitoring oak dieback. Finally, we observed that the S1 features with higher importance tended to be those from winter acquisitions, which can be related to the fact that the leaves are off and the stems and branches are more visible.

The results obtained using the LR algorithm with LASSO penalty leads to the same conclusions (hence, they are not displayed for brevity). In particular, for chestnut, the LR algorithm with LASSO penalty tends to select only 4 features in average (B7, B8A, B6, B11). The feature importance obtained with LASSO penalty for oak is less clear, as in this case good accuracy cannot be achieved with few features. However, additional tests on oak plots using S2 vegetation indices have shown that, on average, good accuracy can be achieved with only 2 or 3 S2 indices and bands. This behavior is probably related to the linear nature of the LR algorithm, which is not the case with the RF algorithm, which can combine the S2 bands in a non-linear way and then rely on fewer features for complex cases.

## V. Conclusion

Our analysis explored the contribution of S1 data to the classification of chestnut and oak dieback. We employed two different classification algorithms, Random Forest and Logistic Regression, on datasets composed of S1 data, S2 data or a combination of both S1 and S2 data. In addition, feature importance was computed based on different techniques (the native RF importance, the SFS method, and the LASSO penalty). Finally, we also demonstrated with the SFS algorithm that only 2 or 3 S2 bands were sufficient to reach a near-optimal accuracy, i.e., bands 7 and 8A are the most important to detect chestnut dieback and band 12 and 8A are the most important to detect oak dieback. This confirm previous findings which had identified the importance of the red-edge and shortwave infrared parts of the S2 spectrum for dieback detection.

Based on our results, we can conclude that the sensitivity of S1 data to forest dieback in oak and chestnut forests is very slight and does not justify the effort and resources required to process and store S1 images, especially for operational systems. From a research perspective, further investigation is needed to determine whether more complex processes could enhance the contribution of S1 data for this application, for example with a better understanding of the relationship between S1 data and tree water content [20]. As a perspective, other specific use cases should be investigated for other species and areas. On the other hand, our findings show that the low sensitivity of S1 to dieback can be used instead in the forest monitoring applications that should not be affected by dieback, such as tree species identification and clear-cut detection.

## Acknowledgments

This work was supported by the SYCOMORE program, with the financial support of the Région Centre-Val de Loire (France), in collaboration with the SuFoSaT project of the GRAINE ADEME program. We thank CNPF and DSF for sharing reference data and CNES for the use of its HPC center.

## References

[1] C. I. Millar and N. L. Stephenson, "Temperate forest health in an era of emerging megadisturbance," *Science*, vol. 349, no. 6250, pp. 823–826, 2015.

[2] F. Mouret, D. Morin, H. Martin, M. Planells, and C. Vincent-Barbaroux, "Toward an operational monitoring of oak dieback with multispectral satellite time series: A case study in Centre-Val de Loire region of France," *IEEE J. Sel. Top. Appl. Earth Obs. Remote Sens.*, vol. 17, pp. 643–659, 2024.

[3] V. Chéret, M. Chartier, J. Denux, J. Julie Vigouroux, and M. Goulard, "Cartographier l'état sanitaire des châtaigniers par télédétection," *Forêt & Innovation*, vol. 2023, no. 1, pp. 20–26, 2023.

[4] H. Abdullah, A. K. Skidmore, R. Darvishzadeh, and M. Heurich, "Sentinel-2 accurately maps green-attack stage of European spruce bark beetle (Ips typographus, L.) compared with Landsat-8," *Remote Sens. Ecol. Conserv.*, vol. 5, no. 1, pp. 87–106, 2019.

[5] S. Valero, L. Arnaud, M. Planells, and E. Ceschia, "Synergy of Sentinel-1 and Sentinel-2 imagery for early seasonal agricultural crop mapping," *Remote Sens.*, vol. 13, no. 23, p. 4891, Dec. 2021.

[6] M. Bruggisser, W. Dorigo, A. Dostálová, M. Hollaus, C. Navacchi, S. Schlaffer, and N. Pfeifer, "Potential of Sentinel-1 C-band time series to derive structural parameters of temperate deciduous forests," *Remote Sens.*, vol. 13, no. 4, p. 798, Feb. 2021.

[7] F. Mouret, M. Albughdadi, S. Duthoit, D. Kouamé, G. Rieu, and J.-Y. Tourneret, "Reconstruction of Sentinel-2 derived time series using robust Gaussian mixture models. Application to the detection of anomalous crop development," *Comput. Electron. Agric.*, vol. 198, p. 106983, 2022.

[8] M. Hollaus and M. Vreugdenhil, "Radar satellite imagery for detecting bark beetle outbreaks in forests," *Curr. Forestry Rep.*, vol. 5, no. 4, p. 240–250, Nov. 2019.

[9] L. Huo, H. J. Persson, and E. Lindberg, "Early detection of forest stress from European spruce bark beetle attack, and a new vegetation index: Normalized distance red & SWIR (NDRS)," *Remote Sens. Environ.*, vol. 255, p. 112240, 2021.

[10] K. Schellenberg, T. Jagdhuber, M. Zehner, S. Hese, M. Urban, M. Urbazaev, H. Hartmann, C. Schmullius, and C. Dubois, "Potential of Sentinel-1 SAR to assess damage in drought-affected temperate deciduous broadleaf forests," *Remote Sens.*, vol. 15, no. 4, p. 1004, 2023.

[11] V. Chéret, M. Chartier, J. Denux, V. J., and G. M, "Cartographier l'état sanitaire des châtaigniers par télédétection," *Forêt & Innovation*, vol. 1, pp. 20–26, 2023.

[12] T. R. Freitas, J. A. Santos, A. P. Silva, and H. Fraga, "Influence of climate change on chestnut trees: A review," *Plants*, vol. 10, no. 7, 2021.

[13] O. Hagolle, M. Huc, D. Villa Pascual, and G. Dedieu, "A multi-temporal and multi-spectral method to estimate aerosol optical thickness over land, for the atmospheric correction of Formosat-2, Landsat, VEN$\mu$S and Sentinel-2 images," *Remote Sens.*, vol. 7, no. 3, pp. 2668–2691, 2015.

[14] X. Blaes, P. Defourny, U. Wegmuller, A. Della Vecchia, L. Guerriero, and P. Ferrazzoli, "C-band polarimetric indexes for maize monitoring based on a validated radiative transfer model," *IEEE Trans. Geosci. Remote Sens.*, vol. 44, no. 4, pp. 791–800, 2006.

[15] R. Nasirzadehdizaji, F. Balik Sanli, S. Abdikan, Z. Cakir, A. Sekertekin, and M. Ustuner, "Sensitivity analysis of multi-temporal sentinel-1 sar parameters to crop height and canopy coverage," *Appl. Sci.*, vol. 9, no. 4, p. 655, 2019.

[16] S. Periasamy, "Significance of dual polarimetric synthetic aperture radar in biomass retrieval: An attempt on sentinel-1," *Remote Sens. Environ.*, vol. 217, pp. 537–549, 2018.

[17] P. Torres, M. Rodes-Blanco, A. Viana-Soto, H. Nieto, and M. García, "The role of remote sensing for the assessment and monitoring of forest health: A systematic evidence synthesis," *Forests*, vol. 12, no. 8, p. 1134, Aug 2021.

[18] F. J. Ferri, P. Pudil, M. Hatef, and J. Kittler, "Comparative study of techniques for large-scale feature selection," in *Machine intelligence and pattern recognition*. Elsevier, 1994, vol. 16, pp. 403–413.

[19] S. Mermoz, J. Doblas Prieto, M. Planells, D. Morin, T. Koleck, F. Mouret, A. Bouvet, D. Sheeren, Y. Hamrouni, T. Belouard, E. Paillassa, M. Carme, M. Chartier, S. Martel, and J.-B. Féret, "Sub-monthly assessment of temperate forest cover and carbon loss in mainland France," *IEEE J. Sel. Top. Appl. Earth Obs. Remote Sens.*, 2024, in press.

[20] I. Pfeil, W. Wagner, M. Forkel, W. Dorigo, and M. Vreugdenhil, "Does ASCAT observe the spring reactivation in temperate deciduous broadleaf forests?" *Remote Sens. Environ.*, vol. 250, p. 112042, Dec. 2020.